

# A highly effective route for removal of Hg<sup>2+</sup> from the waste water using 3-nitrobenzylidenemalononitrile as a modifier of Fe<sub>3</sub>O<sub>4</sub>@SiO<sub>2</sub> nanoparticles

Mosleh Mehryar<sup>1</sup> and Ghasem Marandi\*<sup>2</sup>

<sup>1</sup>Department of Applied Chemistry, Faculty of Chemistry, Urmia University, Urmia, Iran

<sup>2</sup>Department of Organic Chemistry, Faculty of Chemistry, Urmia University, Urmia, Iran

(Received July 2, 2022, Revised September 3, 2023, Accepted November 21, 2023)

**Abstract.** SiO<sub>2</sub>-coated magnetic nanoparticles (Fe<sub>3</sub>O<sub>4</sub>@SiO<sub>2</sub> NPs) were modified by 3-nitrobenzylidenemalononitrile and used as green linkages for removal of Hg<sup>2+</sup> from the wastewater. In this research, it has been attempted to refer to the harmful effects of mercury ions for living things and how to remove such ions using very easy and practical technique. This study shows that by optimizing the test conditions, the efficiency of the removal of harmful ions such as mercury from the water contaminated with these ions can be increased. Conditions such as temperature, speed of agitation, pH of solution were tested for removal of mercury ions. The advantages of this method over other methods listed in the article are the rapid and easy nanocry synthesis. The generated and modified Fe<sub>3</sub>O<sub>4</sub>@SiO<sub>2</sub> nanoparticles were characterized by X-ray diffraction, fourier transform infrared and scanning electron microscopy spectroscopy. The results show that the synthesized magnetic nanoparticles have the excellent performance for the removal of mercury(II) ion from the waste water.

**Keywords:** mercury(II) ion removal; modified magnetic nanoparticles; 3-nitrobenzylidenemalononitrile

## 1. Introduction

In recent years, the diffusion of heavy metal ions is a serious problem for humans and their environment (Qasem *et al.* 2021). This dissemination is mostly due to population development and industrialization of communities and the growing need to use new products and produce more waste. Heavy metal ions such as mercury could be carcinogenic because they are non-biodegradable (Prabhu *et al.* 2018). Therefore, the entry of these ions into the living environment of organisms, even on a very small scale, can create irreparable dangers (Zou *et al.* 2016, Velusamy *et al.* 2021). The solubility of these ions in aqueous solutions causes to have a high potential to penetrate the living environment of organisms and pose risks such as poisoning and cancer (Mitra *et al.* 2022), (see Fig. 1). For example, the solubility of mercuric chloride at 25 °C in water is 69 g/Lit (Leeuwrn *et al.* 2000).

There are many techniques for the treatment of wastewater from the heavy metals such as chemical precipitation, ion exchange, adsorption, membrane filtration, coagulation and flocculation, flotation, and electrochemical treatment (Fu *et al.* 2011), but one of the most effective, interesting, and new ways could be nanosynthetic adsorbents with modified structures via organic compounds.

In recent years, utility advantages of Fe<sub>3</sub>O<sub>4</sub>@SiO<sub>2</sub> nanoparticles such as easy preparing and coating, low cost generation, ability of control on surface modification, absorption on nanoscale diameters and easy separation

techniques (Machala *et al.* 2007, Aryn *et al.* 2009) have caused to increasing use of them (Ahmad *et al.* 2018). Due to the presence of hydroxyl groups on the surfaces of hydrophobic nanoparticles, it is possible to graft some types of organic or inorganic molecules to modify the surfaces of nanoparticles, which can be used to absorb various types of ions (Manna *et al.* 2012). Direct or indirect linkage of some organic molecules to the surface of nanoparticles can create good and effective biocompatibility for the isolation of biologically active compounds (Pan *et al.* 2010, Ahmad *et al.* 2019). In addition to items that mentioned above, other parameters such as solution pH, nanoparticle size, temperature, duration of material contact on the nanoparticle surface, can affect in the absorption of ions or molecules by nanoparticles (Ahmad *et al.* 2019, Jasrotia *et al.* 2022).

Therefore, in respect to the importance of environmental problems dissolving, we decided to investigate the synthesis of modified Fe<sub>3</sub>O<sub>4</sub>@SiO<sub>2</sub> nanoparticles via 3-nitrobenzylidenemalononitrile for the removal of Hg<sup>2+</sup> (Zhang *et al.* 2014). The interesting aspect of this procedure is not only the absence of expensive instrumental techniques such as atomic fluorescence spectrometry, etc. (Hu *et al.* 2013, Leopold *et al.* 2008, Zhang *et al.* 2015), but also the use of nanomagnetic compounds coated with organic compounds containing the cyanide functional group to separate mercury (II) ions (Baby *et al.* 2019).

On the base of the literature survey, the adsorption protocol is one of the cheaper procedures among the remediation methods and a really efficient and advantageous method for removing heavy metal ions (Zou *et al.* 2016, Velusamy *et al.* 2021).

The binding ability of the -C≡N functional group to the metal ions gave us an opportunity to use 3-nitrobenzylidenemalononitrile for the synthesis of modified

\*Corresponding author, Professor,  
E-mail: marandi\_gh@yahoo.com; g.marandi@urmia.ac.ir

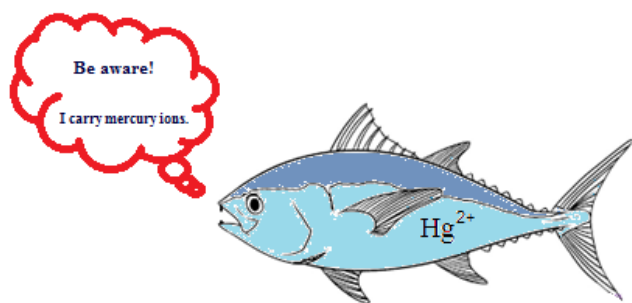


Fig. 1 The entry of heavy metal ions into the life cycle of animals and humans

$\text{Fe}_3\text{O}_4@/\text{SiO}_2$  nanoparticles for the removal of mercury(II) ions from the wastewater (Girgis *et al.* 2015).

One of the main attractions of using  $\text{Fe}_3\text{O}_4$  nanoparticles in the synthesis of chemical compounds is their separation by an external magnetic field. Therefore, for the first time, we used the same property to separate mercury ions in water. It should be noted, however, that the nanocomposite particles were coated using 3-nitrobenzylidenemalononitrile which had a high ability to bind to the mercury (II) ions (Lee *et al.* 2013, Nookala *et al.* 2015).

## 2. Experimental

### 2.1 Material and methods

All chemicals have been purchased from Merck, Sigma Aldrich and Fluka Companies and were used without further purification. The FT-IR spectra were recorded on a TENSOR II Model Bruker spectrometer. Also, the  $^1\text{H}$  NMR spectrum for the 3-nitrobenzylidenemalononitrile was recorded on a BRUKER DRX-250 AVANCE instrument using  $\text{CDCl}_3$  as a solvent and TMS as internal standard at 250 MHz. X-ray diffraction (XRD) patterns were recorded by using a XRD PW1730 Philips an X-ray diffractometer using a  $\text{Cu K}_\alpha$  anode. Scanning electron microscopy (FE-SEM) images were obtained on ZEISS LEO 1430 VP instrument operated at 30 kV accelerating voltage. All the UV-Vis absorption spectra measurements were carried out in the 200-600 nm region using a UV600-Shimadzu UV-vis spectrophotometer with a 10 mm light-path black quartz spectrophotometer cell. The melting point of synthesized 3-nitrobenzylidenemalononitrile was recorded on a Barnstead Electrothermal 9200 apparatus. The stock solution of  $\text{Hg}^{2+}$  ( $1.0 \times 10^{-3}$  M) was prepared by dissolving of  $\text{Hg}(\text{NO}_3)_2$  in deionized water and a series of standard solutions of  $\text{Hg}^{2+}$  were prepared by stepwise diluting of stock solution.

### 2.2 Synthesis of 3-nitrobenzylidenemalononitrile

A magnetically stirred solution of 3-nitrobenzaldehyde (2 mmol) in ethanol (5 mL) was added a solution of malononitrile (2 mmol) in (5 mL) over 5 min at room temperature. After the addition of malononitrile, the reaction mixture was stirred for 6 hours at room temperature. The progress of the reaction was monitored by

TLC in the solvent combination ethylacetate/*n*-hexane (2:8) as the mobile phase. After the completion of the reaction, the solvent was evaporated and the resulting precipitate was washed with ( $3 \times 2$  mL) of cold diethyl ether. The crude product has been recrystallized from ethanol (5 mL) to afford the pure 3-nitrobenzylidenemalononitrile.

### 2.3 Synthesis of modified $\text{Fe}_3\text{O}_4@/\text{SiO}_2$ nanoparticles as absorbent of $\text{Hg}^{2+}$ ion

A surface modification strategy was used for the successful synthesis of  $\text{Fe}_3\text{O}_4@/\text{SiO}_2$  which has shown in Scheme 1 (Zare *et al.* 2020, Qu *et al.* 1999). At the first step, 20 mmol of  $\text{FeCl}_3 \cdot 6\text{H}_2\text{O}$  and 10 mmol of  $\text{FeCl}_2 \cdot 4\text{H}_2\text{O}$  were added to 50 mL of distilled  $\text{H}_2\text{O}$  in a flask at room temperature, then the reaction mixture warms up to 80 °C. After that, the reaction mixture was brought to pH 10 by dropwise addition of NaOH (3 M). All reaction mixture stirred under  $\text{N}_2$  atmosphere for 12 h. The black solid phase has been collected by a centrifuge and washed using deionized water. In the next step, 1 g of  $\text{Fe}_3\text{O}_4$  was added to a mixture of ethanol (50 ml) and deionized water (5 ml), then, 25% ammonia solution (2 mL) was added to the reaction mixture. Then, 2 mL of tetraethyl orthosilicate (TEOS) was added dropwise to the mixture and was allowed to stir for 3 hours at 60 °C. The magnetic material is then collected again and washed with a mixture of water/ethanol (1:1) and then dried at 50 °C. In the last part, to prepare the adsorbent, 1 g of the obtained magnetic cores was added in a mixture of acetone (20 mL) as a solvent and 3-nitrobenzylidenemalononitrile (1 mmol), and then the reaction mixture was stirred for 24 hours at 50 °C. In the final step of adsorbent generation, the solvent was removed and the residues were dried at room temperature for 24 hours. (Fig. 2)

## 3. Results and discussion

A simple well-known Knoevenagel condensation reaction has been used to synthesize of 3-nitrobenzylidenemalononitrile as an absorbent layer on the surface of nanoparticles (Zengin *et al.* 2020, Jadhav *et al.* 2019, Carvalho *et al.* 2018, Marandi *et al.* 2011).

The synthesized stable structure of 3-nitrobenzylidenemalononitrile was deduced from its spectroscopic data such as  $^1\text{H}$  NMR and IR spectroscopy (see Fig. 3). The FT-IR spectrum of synthesized 3-nitrobenzylidenemalononitrile show a peak at  $2213 \text{ cm}^{-1}$  for  $-\text{C}\equiv\text{N}$  group and  $-\text{NO}_2$  group shows vibration signals at  $1374$  and  $1449 \text{ cm}^{-1}$  and also,  $^1\text{H}$  NMR spectrum shows that all protons of olefinic and aromatic moieties resonate between 7.71 and 8.45 ppm.

Different analytical techniques have been used for the characterization of  $\text{Fe}_3\text{O}_4@/\text{SiO}_2@/3$ -nitrobenzylidenemalononitrile NPs such as XRD, SEM, and IR.

The FT-IR spectrum of naked  $\text{Fe}_3\text{O}_4$  shows strong peak at  $617 \text{ cm}^{-1}$  and it is attributed to the Fe-O band and also, the existence of broad peaks at  $3000$ - $3400 \text{ cm}^{-1}$  is according to the structure of  $\text{Fe}_3\text{O}_4$  and indicates the symmetric and asymmetric vibration modes of OH bonds which are linked

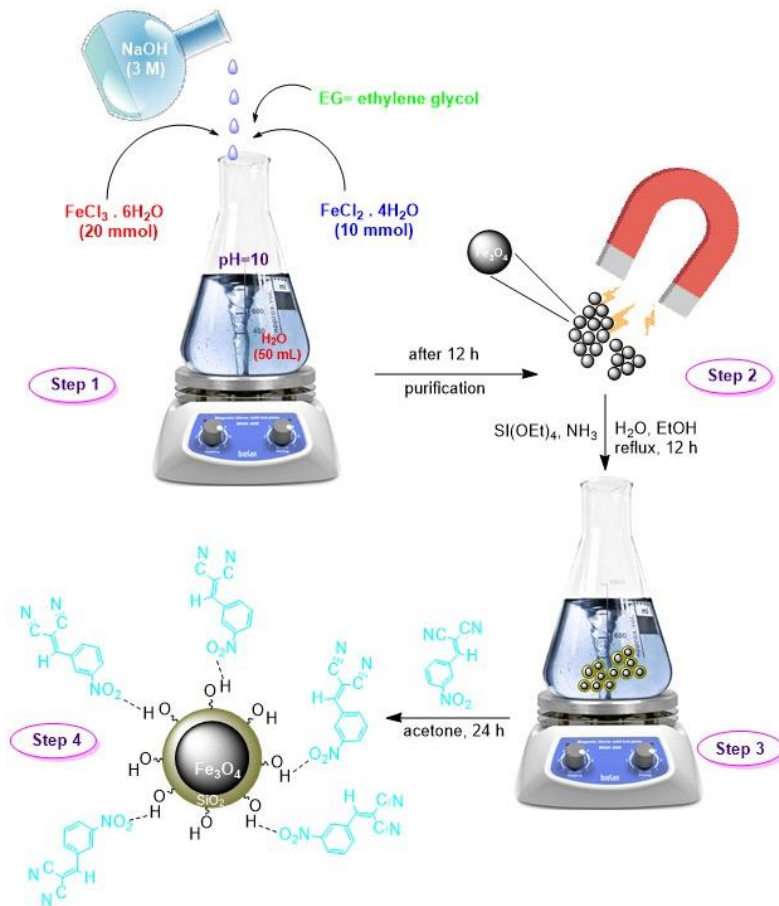


Fig. 2 Synthesis of modified  $Fe_3O_4@SiO_2$  nanoparticles as  $Hg^{2+}$  absorbent

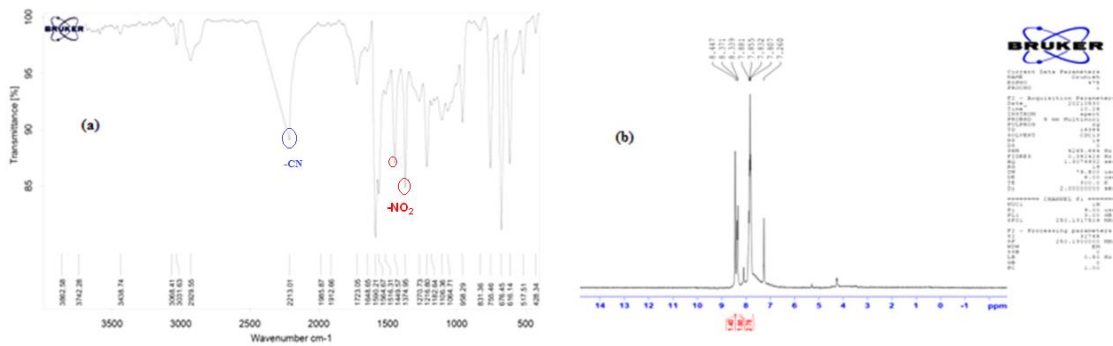


Fig. 3 (a) FT-IR and (b)  $^1H$  NMR spectra of synthesized 3-nitrobenzylidenemalononitrile

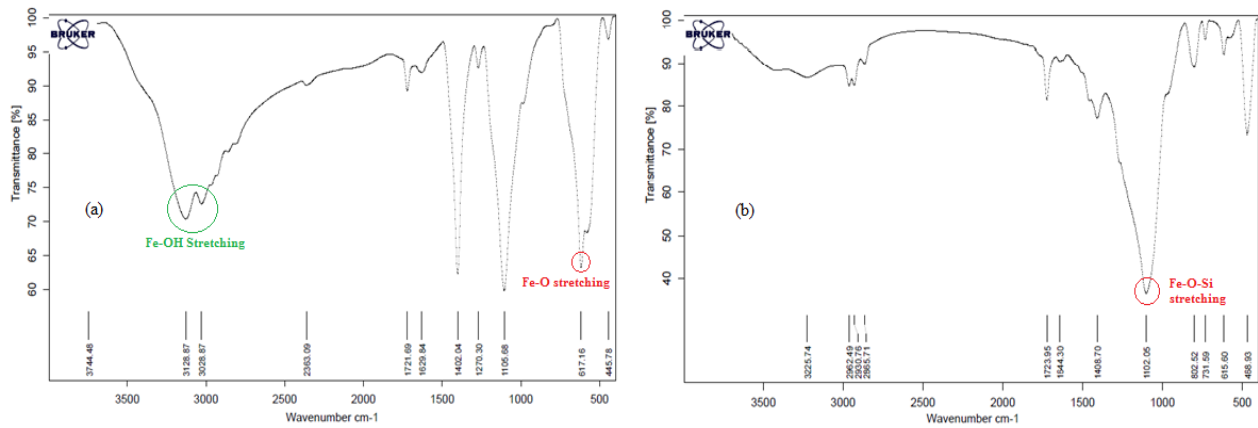


Fig. 4 FT-IR spectra of (a) naked  $Fe_3O_4$  NPs, (b) silica coated  $Fe_3O_4$  NPs

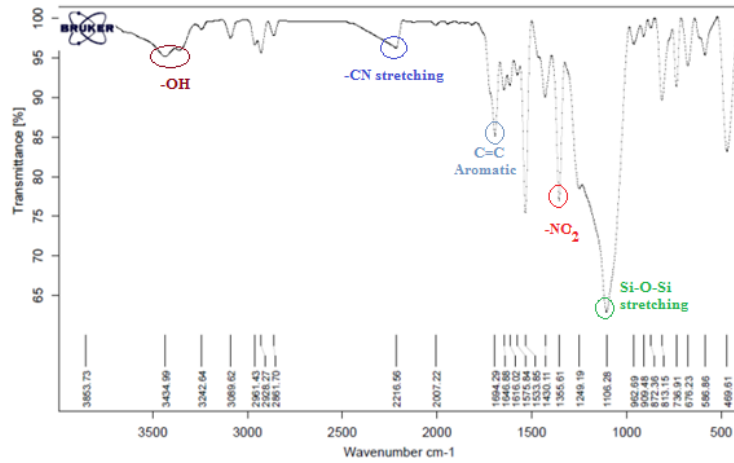


Fig. 5 FT-IR of modified silica coated  $\text{Fe}_3\text{O}_4$  NPs

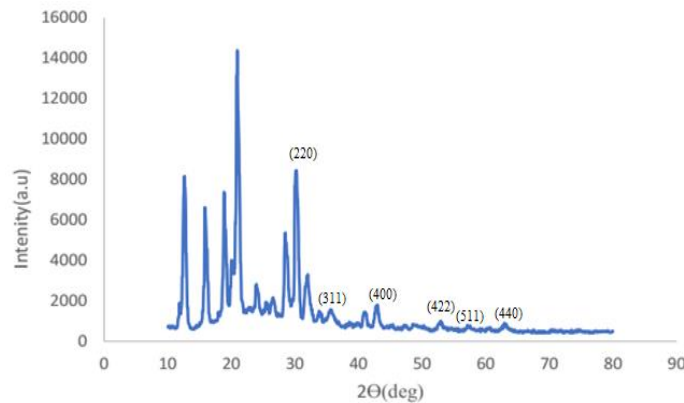


Fig. 6 The XRD pattern of nano-absorbent

to the surface of  $\text{Fe}_3\text{O}_4$  NPs. After that the surface of  $\text{Fe}_3\text{O}_4$  NPs is coated by  $\text{SiO}_2$ , its FT-IR spectrum exhibits a strong peak at  $1102\text{ cm}^{-1}$  and which is attributed to Fe-O-Si stretching vibration mode (Gemeay *et al.* 2020) (see Fig. 4).

After the modification of the surface of  $\text{Fe}_3\text{O}_4$  NPs via 3-nitrobenzylidenemalononitrile, its FT-IR spectrum shows characteristic peaks at  $2216\text{ cm}^{-1}$  for  $-\text{C}\equiv\text{N}$ ,  $1355, 1533\text{ cm}^{-1}$  for symmetric and asymmetric vibration of  $-\text{NO}_2$  groups and also peak at  $1106.28$  attributed to stretching vibration of Si-O-Si, respectively (Fig. 5).

The FT-IR results show that both the silica as coating of  $\text{Fe}_3\text{O}_4$  NPs and the synthesized organic compound, 3-nitrobenzylidenemalononitrile are present as adsorbents on the surface of nanoparticles.

Moreover, information obtained from X-ray diffraction (XRD) analysis of synthesized nanoparticles is in good agreement with the standard  $\text{Fe}_3\text{O}_4$  patterns which were reported in literature (Zare *et al.* 2020, 2019).

The diffraction peaks at  $2\theta = 28.54, 30.14, 32.14, 35.10, 41.45, 50.65, 63.25$  are observed in the XRD diagram and are related to  $\text{Fe}_3\text{O}_4$  and a broadened area has been seen at  $2\theta = 15\text{--}25^\circ$  in this XRD pattern and it can belong to amorphous  $\text{SiO}_2$  layer (Fig. 6). The peaks (220), (311), (400), (422), (511) and (440) are characteristic peaks of as standard  $\text{Fe}_3\text{O}_4$  sample (Wang *et al.* 2018). However, in

according to XRD pattern, it can be said that most of the peaks indicate that the nanoparticles are amorphous nanoparticles (Mobinikhaledi *et al.* 2018, Yao *et al.* 2014, Farooq *et al.* 2020).

The morphology of the synthesized magnetic nanoparticles was investigated using field emission scanning electron microscopy (FE-SEM) and the results show that the synthesized absorbent MNPs with a size under  $100\text{ nm}$  have been done (Fig. 7). However, it should be mentioned that due to the aggregation of the particles with paramagnetic nature, it is also possible for nanoparticles to clump. This phenomenon is seen in part (c) of Fig 7. for synthesized  $\text{Fe}_3\text{O}_4$  NPs.

The Energy Dispersive X-ray (EDX) experiment of the nanoparticle shows that Fe, Si and O elements are present in the structure of the nanoparticle. However, it should be mentioned that there is a small amount of S atom as impurity next to these elements with corresponding weight percents  $13.40\%, 33.36\%, 52.24\%$  and  $1.00\%$ , respectively (Fig. 8).

After the synthesis and characterization of the nanoparticle, the absorbent moiety was placed on the nanoparticle shell. The final nanocomposite was then used to adsorb mercury (II) ions. The illustrative figure below shows how the synthesized nanomaterial works as  $\text{Hg}^{2+}$

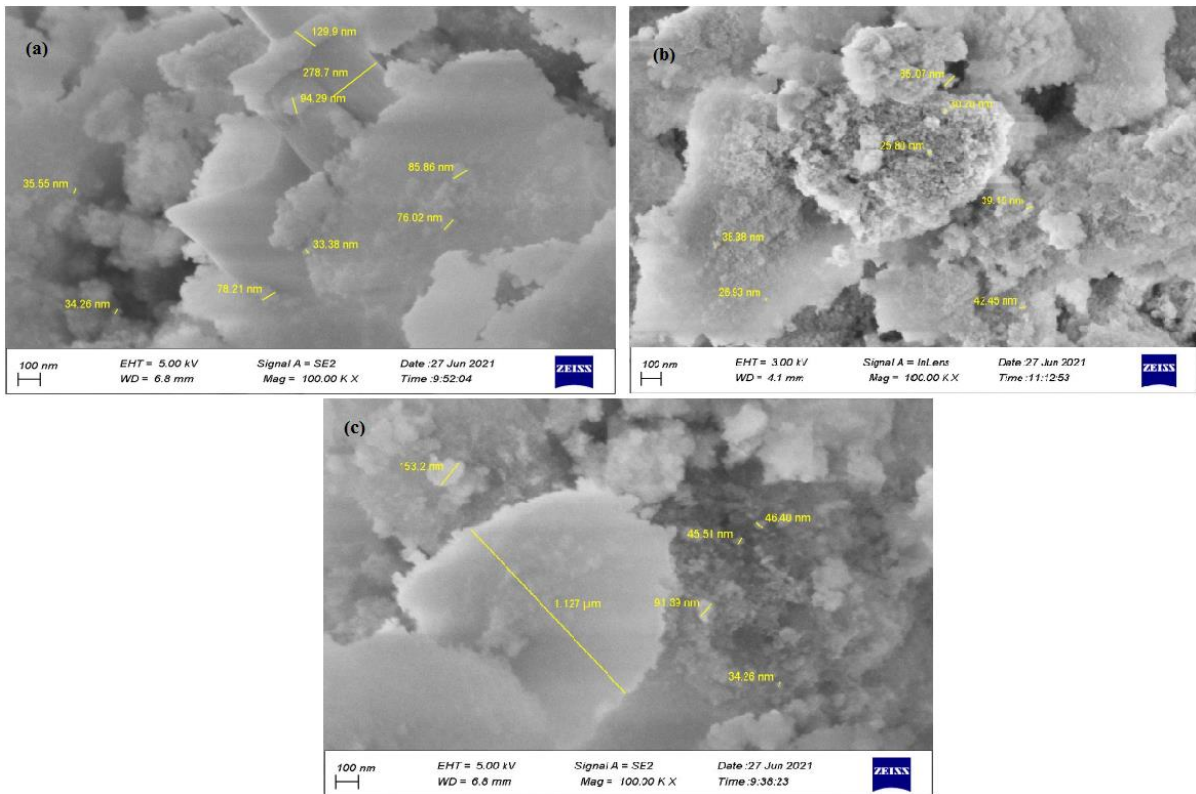


Fig. 7 The FE-SEM images of magnetic nanoparticles

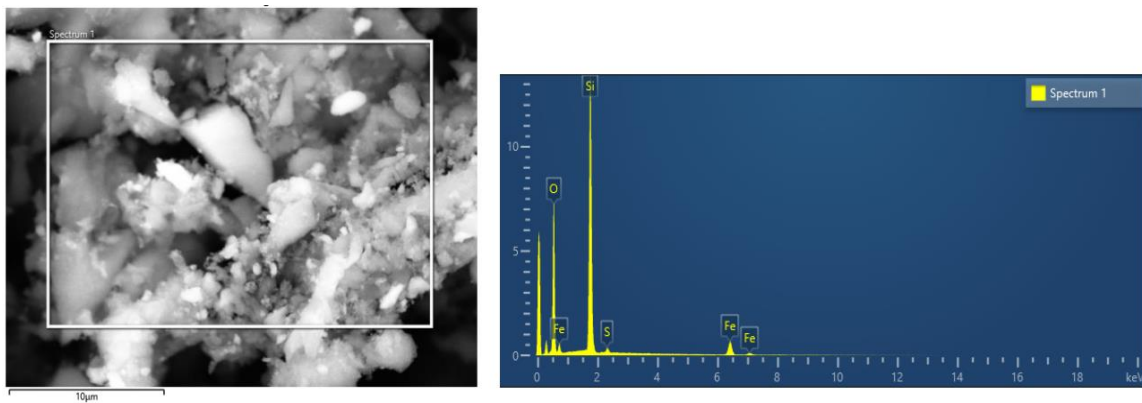


Fig. 8 SEM and EDX spectrum of  $Fe_3O_4@SiO_2$  NPs

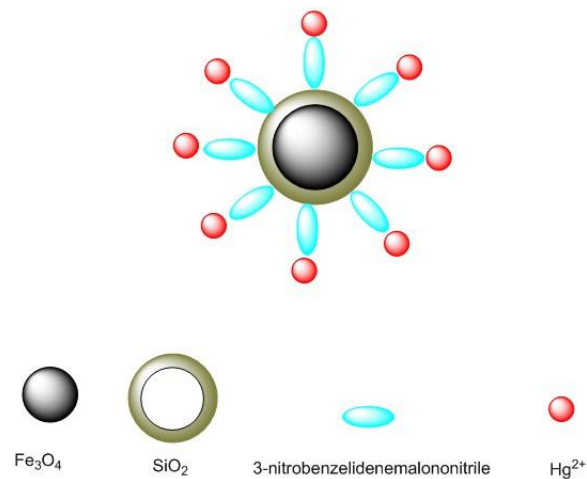


Fig. 9 A proposed route for  $Hg^{2+}$  ions adsorption by the synthesized nanocomposites

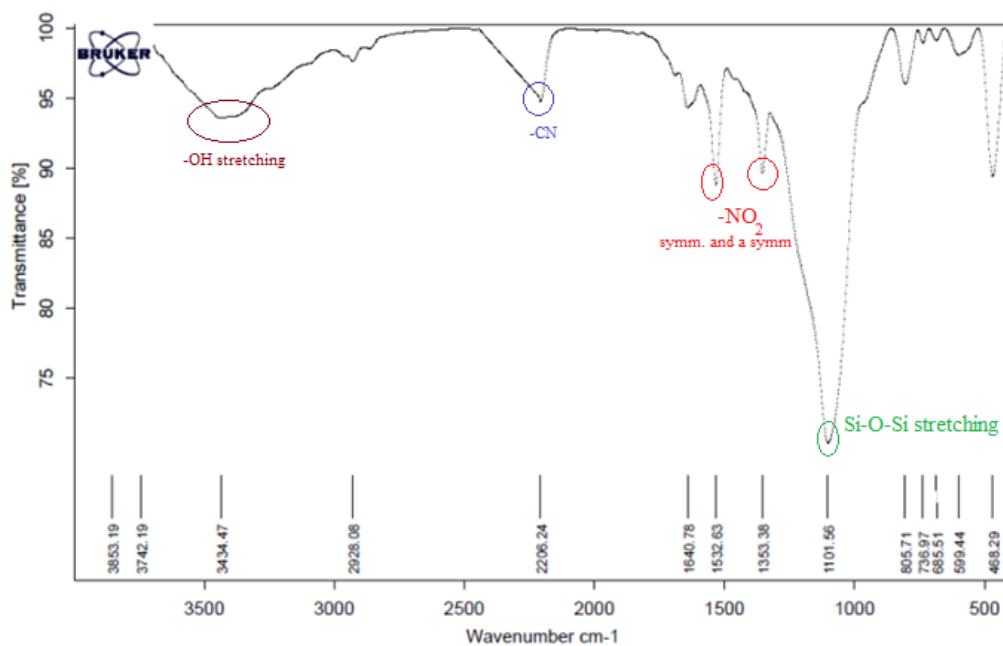


Fig. 10 The FT-IR spectrum of synthesized nanocomposites after the absorption of  $\text{Hg}^{2+}$  ions

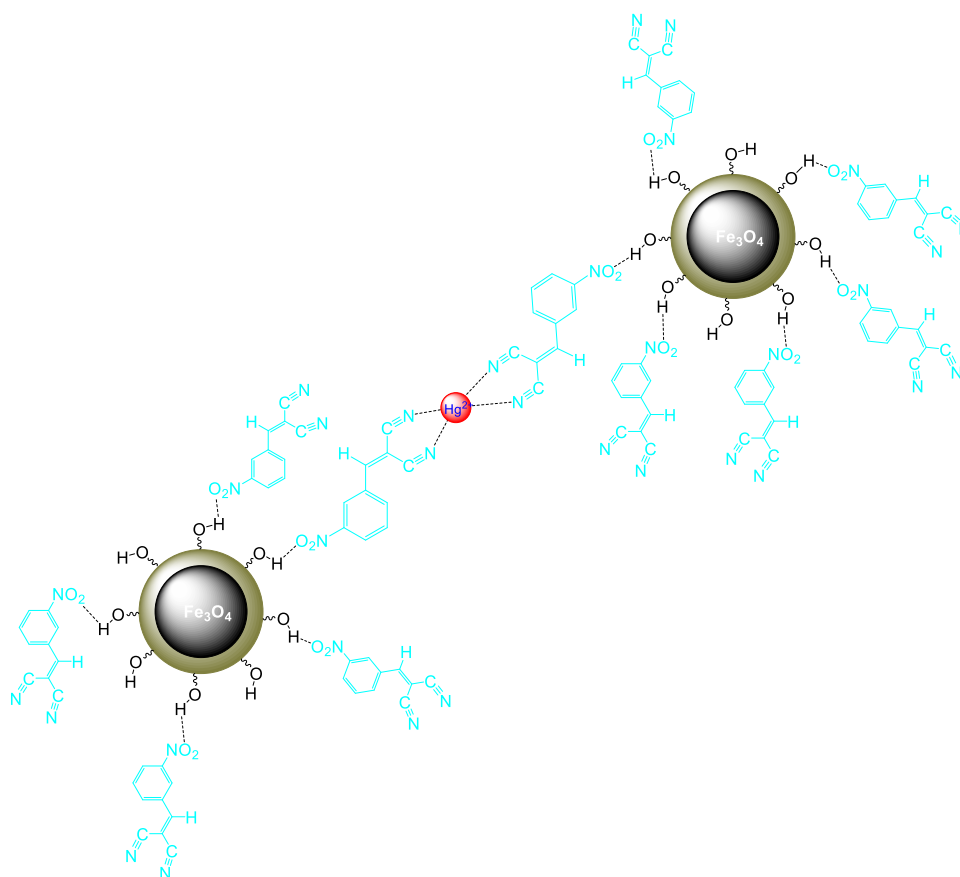


Fig. 11 an acceptable route for absorption of  $\text{Hg}^{2+}$  ions by synthesized nano-absorbent

ions absorbent (Fig. 9). After the proving of the synthesis of the nano-absorbent, its absorption activity was investigated using a 0.1 M solution of  $\text{Hg}(\text{NO}_3)_2$ . The FT-IR spectrum of nano-particles after the adsorption of  $\text{Hg}^{2+}$  ions from a 0.1 M solution of  $\text{Hg}(\text{NO}_3)_2$  shows a characteristic peak at 2206

$\text{cm}^{-1}$  (Fig. 10) which is attributed to  $-\text{C}\equiv\text{N}$  and the difference between before and after absorption indicates the possibility of cyanide groups being involved with mercury ions. This decreases in wave number ( $\Delta\nu_{-\text{C}\equiv\text{N}} = 10 \text{ cm}^{-1}$ ) in malonitrile moiety after absorption of mercury ions can

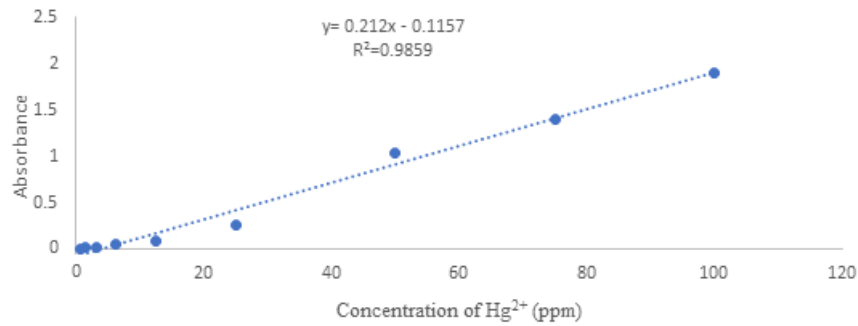


Fig. 12 The calibration curve of the mercury ions in terms of concentration at 25 °C

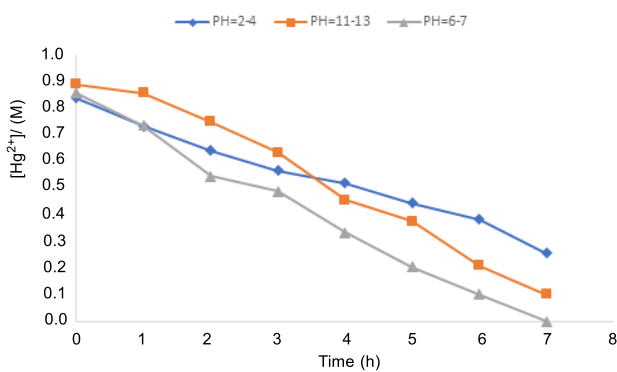


Fig. 13 Effect of pH on absorption of  $\text{Hg}^{2+}$  by nano-absorbent at 25 °C

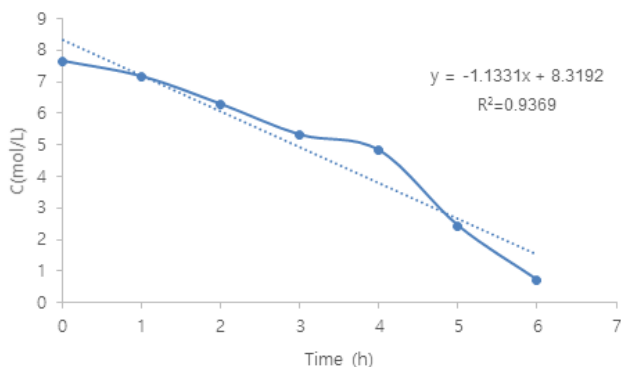


Fig. 14 The effect of absorption time to absorb  $\text{Hg}^{2+}$  ions by nano-absorbent

be attributed to the back-donation of an electron pair from the metal to one  $\pi^*$  orbital of the nitrile group (Storhoff *et al.* 1977, Bresciani *et al.* 2021). This interaction between  $\text{Hg}^{2+}$  and cyanide groups shows that synthesized absorbent has a high potential to removing of mercury(II) ion.

Fig. 11 shows one of the acceptable routes for absorption of  $\text{Hg}^{2+}$  ions in the presence of a nano-absorbent. Although, another plausible mechanism can exist for the removal of  $\text{Hg}^{2+}$  ions (see Fig. 11).

In the following, to obtain the optimal procedure conditions for the best absorption, some parameters such as absorption time, pH, temperature, and agitation speed were evaluated and the results were presented.

In the first step, to calibrate and draw the plot of the absorbance changes in terms of concentration of  $\text{Hg}^{2+}$  in  $\lambda_{\text{max}}$  (525 nm), for this purpose, standard solutions (0.3-100

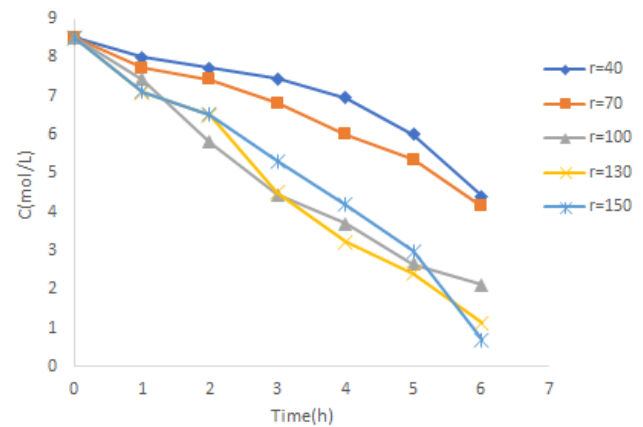


Fig. 15 The effect of speed of agitation on absorption of  $\text{Hg}^{2+}$  ions by nano-absorbent

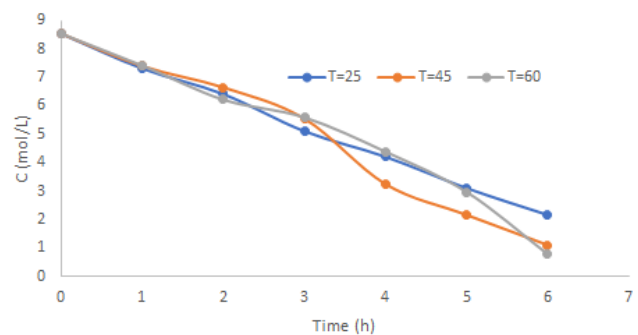


Fig. 16 The effect of Temperature on absorption of  $\text{Hg}^{2+}$  by nano-absorbent

ppm) of  $\text{Hg}(\text{NO}_3)_2$  were prepared and experimented under neutral conditions at room temperature. Fig. 12 shows the calibration graph of the mercury ions.

After the calibration of the system, the effect of pH on the absorption of  $\text{Hg}^{2+}$  by absorbent was studied at 25 °C.

The experiments were performed at different pHs (2-4), (6-7) and (11-13), and as shown in Fig. 13, the highest amount of absorption of  $\text{Hg}^{2+}$  ions occurred in environments with pH 6-7.

Another parameter that highly influences the absorption of  $\text{Hg}^{2+}$  ions in this procedure is the absorption time. Fig. 14 shows that after 6 hours the highest amount of  $\text{Hg}^{2+}$  ions are absorbed by the nano-absorbent. It seems to be true that the more contact time of the nano-adsorbent with the  $\text{Hg}^{2+}$  ions, the more ions are absorbed by the nano-adsorbent.

Table 1 The absorption performance of nano-absorbent in various conditions

Absorbent	Absorbed ion	Conditions						Remarks
		pH	capacity (mol/L)	stirred speed (rpm)	capacity (mol/L)	Temperature (°C)	capacity (mol/L)	
Modified Fe <sub>3</sub> O <sub>4</sub> NPs	Hg <sup>2+</sup>	2-4	5.806	40	4.1	25 45 60	6.37 7.43 7.752	The best conditions for Hg <sup>2+</sup> removal by modified silica coated Fe <sub>3</sub> O <sub>4</sub> NPs are under neutral pH, stirred speed 150 rpm and 60 °C conditions.
		6-7	7.889	100	6.36			
				130	7.39			
		11-13	5.562	150	7.814			

To optimize this procedure, the speed of agitation for absorption of Hg<sup>2+</sup> ions was investigated. It was found that the range of stirrer speed can affect the absorption of Hg<sup>2+</sup> ions by nano-absorbent. Additional experiments were carried out at 40, 70, 100, 130, and 150 rpm. The experiments show that among the mentioned stirred speeds, the speed of 150 rpm has the best performance for absorption of Hg<sup>2+</sup> ions (Fig. 15).

Temperature parameter for this procedure in another series of experiments was studied and the results showed that nano-absorbent at 60 °C has the excellent performance among the 25, 45 and 60 °C (Fig. 16).

Table 1. shows the results of Hg<sup>2+</sup> ion absorption experiments in different conditions such as pH, temperature and stirring speed.

#### 4. Conclusions

In summary, we describe an interesting route for the removal of Hg<sup>2+</sup> ion as one of the extra harmful and toxic ions with high pathogenic potential from the wastewaters. Synthesized Fe<sub>3</sub>O<sub>4</sub> bearing nano-absorbents have a rapid performance to remove of Hg<sup>2+</sup> ion which its function is excellent in comparison to the other spectroscopic methods. The experimental results show that the best performance for modified Fe<sub>3</sub>O<sub>4</sub> MNPs was occurred in neutral pH, stirred speed 150 rpm and 60 °C. It should be mentioned that the use of 3-nitrobenzylidenemalononitrile supported on Fe<sub>3</sub>O<sub>4</sub> MNPs is the first facile, non-toxic and non-expensive method for the removal of Hg<sup>2+</sup> ions from the wastewater.

#### Acknowledgments

The authors would like to thank the Urmia University research council for partial financial support of this work.

#### References

- Ahmad, I. Siddiqui, W.A. Qadir, S. and Ahmad, T. (2018), "Synthesis and characterization of molecularly imprinted nanomaterials for the removal of heavy metals from water", *J. Mater. Res. Technol.*, **7**, 270-282. <https://doi.org/10.1016/j.jmrt.2017.04.010>.
- Ahmad, I. Siddiqui, W.A. Ahmad, T. and Siddiqui, V.U. (2019), "Synthesis and characterization of molecularly imprinted ferrite (SiO<sub>2</sub>@Fe<sub>2</sub>O<sub>3</sub>) nanomaterials for the removal of nickel (Ni<sup>2+</sup> ions) from aqueous solution", *J. Mater. Res. Technol.*, **8**, 1400-1411. <https://doi.org/10.1016/j.jmrt.2018.09.011>.
- Ahmad, I. Siddiqui, W.A. and Ahmad, T. (2019), "Synthesis and characterization of molecularly imprinted magnetite nanomaterials as a novel adsorbent for the removal of heavy metals from aqueous solution", *J. Mater. Res. Technol.*, **8**, 4239-4252. <https://doi.org/10.1016/j.jmrt.2019.07.034>.
- Baby, R. Saifullah, B. and Husseian, M.Z. (2019), "Carbon nanomaterials for the treatment of heavy metal-contaminated water and environmental remediation", *Nanoscale Res. Lett.*, **14**, 341-357. <https://doi.org/10.1186/s11671-019-3167-8>.
- Bresciani, G. Biancalana, L. Pampaloni, G. Zacchini, S. Ciancaleoni, G. and Marchetti, F. (2021), "A comprehensive analysis of the metal–nitrile bonding in an organo–diiron system", *Molecules*, **26**, 7088-7114. <https://doi.org/10.3390/molecules26237088>.
- Carvalho, H.L. Amorim, A.L. Araújo, I.F. Marino, B.L.B. Jimenez, D.E.Q. Ferreira, R.M.A. Hage-Melim, L.I.P. Souto, R.N.S. Porto, A.L.M. and Ferreira, I.M. (2018), "A Simple and efficient protocol for the Knoevenagel reaction of benzylidene-malononitriles and the evaluation of the larvicidal activity on *Aedes Aegypti*", **10**, 362-374. <https://doi.org/10.21577/1984-6835.20180028>.
- Farooq, U. Chaudhary, P. Ingole, P.P. Kalam, A. and Ahmad, T. (2020), "Development of cuboidal KNbO<sub>3</sub>@α-Fe<sub>2</sub>O<sub>3</sub> hybrid nanostructures for improved photocatalytic and photoelectron-catalytic applications", *ACS Omega*, **5**, 20491-2050. <https://doi.org/10.1021/acsomega.0c02646>.
- Fu, F. and Wang, Q. (2011), "Removal of heavy metal ions from wastewaters: a review", *J. Environ. Manage.*, **92**, 407-418. <https://doi.org/10.1016/j.jenvman.2010.11.011>.
- Gemeay, A.H. Keshta, B.E. El-Sharkawy, R.G. and Zaki, A.B. (2020), "Chemical insight into the adsorption of reactive wool dyes onto amine-functionalized magnetite/silica core-shell from industrial wastewaters", *Environ. Sci. Pollut. Res.*, **27**, 32341-32358. <https://doi.org/10.1007/s11356-019-06530-y>.
- Girgis, E. Adel. D. Tharwat, C. Attallah, O. and Rao, K.V. (2015), "Cobalt ferrite nanotubes and porous nanorods for dye removal", *Adv. Nano. Res.*, **3**(2), 111-121. <http://doi.org/10.12989/anr.2015.3.2.111>.
- Hu, B. Hu, L.L. Chen, M.L. and Wang, J.H. (2013), "A FRET ratiometric fluorescence sensing system for mercury detection and intracellular colorimetric imaging in live Hela cells", *Biosens. Bioelectron.*, **49**, 499-505. <https://doi.org/10.1016/j.bios.2013.06.004>.
- Jadhav, A.L. and Yadav, G.D. (2019), "Clean synthesis of benzylidenemalononitrile by Knoevenagel condensation of benzaldehyde and malononitrile: effect of combustion fuel on activity and selectivity of Ti-hydroxalcalite and Zn-hydroxalcalite catalysts", *J. Chem. Sci.*, **131**, 79-93. <https://doi.org/10.1007/s12039-019-1641-6>.
- Jasrotia, R. Suman, Verma, A. Verma, R. Ahmed, J. Godara, S.K. Mehtab, A. Ahmad, T. and Kalia, S. (2022), "Photocatalytic dye degradation efficiency and reusability of Cu-substituted Zn-Mg spinel nanoferrites for wastewater remediation", *J. Water Proc. Eng.*, **48**, 102865. <https://doi.org/10.1016/j.jwpe.2022.102865>.
- Lee, E.M. Gwon, S.Y. Kim, S.H. (2014), "Spectral properties of

- highly selective chemosensor for Hg<sup>2+</sup>”, *Spectrochim. Acta A Mol. Biomol. Spectrosc.*, **120**, 646-649.  
<http://doi.org/10.1016/j.saa.2013.10.061>.
- Leeuwen, F.X.R. and Krzyzanowski M. (2000), *World Health Organization. Regional Office for Europe, Air quality guidelines for Europe*, WHO, Copenhagen, Netherlands.
- Leopold, K. Harwardt, L. Schuster, and M. Schlemmer, (2008), “A new fully automated on-line digestion system for ultra trace analysis of mercury in natural waters by means of FI-CV-AFS”, *Talanta*, **76**, 382-388.  
<https://doi.org/10.1016/j.talanta.2008.03.010>.
- Machala, J. Zboril, R. and Gedanken, A. (2007), “Amorphous iron(III) oxides: A review”, *J. Phys. Chem. B*, **111**, 4003-4018.  
<https://doi.org/10.1021/jp064992s>.
- Manna, U. Broderick, A.H. Lynn, and D.M. (2012), “Chemical patterning and physical refinement of reactive superhydrophobic surfaces”, *Adv. Mater.* **24**, 4291-4295.  
<https://doi.org/10.1002/adma.201200903>.
- Marandi, G. Maghsoodlou, M.T. Hazeri, N. Habibi-Khorassani, S.M. Akbarzadeh-Torbati, N. Rostami-Cherati, F. Skelton, B.W. and Makha, M. (2011), “Synthesis of cyano-2,3-dihydropyrrolo[1,2-f]phenanthridine derivatives via a domino-Knoevenagel-cyclization”, *Mol. Divers.*, **15**, 197-201.  
<https://doi.org/10.1007/s11030-010-9254-5>.
- Mitra, S. Chakraborty, A.J. Tareq, A.M. Bin Emran, T. Nainu, F. Khusro, A. Idris, A.M. Khandaker, M.U. Osman, H. Alhumaydhi, F.A. and Simal-Gandara, J. (2022), “Impact of heavy metals on the environment and human health: Novel therapeutic insights to counter the toxicity”, *J. King Saud Univ. Sci.*, **34**, 101865. <https://doi.org/10.1016/j.jksus.2022.101865>.
- Mobinkhaleli, A. Moghanian, H. Hosseini-Gazvini, S.M.B. and Dalvand, A. (2018), “Copper containing poly(melamine-terephthaldehyde)-magnetite mesoporous nanoparticles: a highly active and recyclable catalyst for the synthesis of benzimidazole derivatives”, *J. Porous Mater.*, **25**, 1123-1134.  
<https://doi.org/10.1007/s10934-017-0524-9>.
- Nookala, S. Tollamadugu, N.V.K.V.P. Thimmavajjula, G.K. and Ernest, D. (2015), “Effect of citrate coated silver nanoparticles on biofilm degradation in drinking water PVC pipelines”, *Adv. Nano. Res.*, **3**, 97-109.  
<http://doi.org/10.12989/anr.2015.3.2.097>.
- Pan, B. Qiu, H. Pan, B. Nie, G. Xiao, L. Lv, L. Zhang, W. Zhang, Q. and Zheng, S. (2010), “Highly efficient removal of heavy metals by polymer-supported nanosized hydrated Fe(III) oxides: Behavior and XPS study”, *Water Res.*, **44**, 815-824.  
<https://doi.org/10.1016/j.watres.2009.10.027>.
- Prabhu, P.P. and Prabhu, B. (2018), “A review on removal of heavy metal ions from waste water using natural/ modified bentonite”, *MATEC Web of Conferences*, **144**, 02021, 1-13.  
<https://doi.org/10.1051/mateconf/201814402021>.
- Qasem, N.A.A. Mohammed, R.H. and Lawal, D.U. (2021), “Removal of heavy metal ions from wastewater: A comprehensive and critical review”, *npj Clean Water*, **4**, 36, 1-15. <https://doi.org/10.1038/s41545-021-00127-0>.
- Qu, S. Yang, H. Ren, D. Kan, S. Zou, G. Li, D. and Li, M. (1999), “Magnetite nanoparticles prepared by precipitation from partially reduced ferric chloride aqueous solutions”, *J. Colloid Interf. Sci.*, **215**, 190-192.  
<https://doi.org/10.1006/jcis.1999.6185>.
- Storhoff, B.N. Lewis, H.C. Jr. (1977), “Organonitrile complexes of transition metals”, *Coord. Chem. Rev.*, **23**, 1-29.  
[https://doi.org/10.1016/S0010-8545\(00\)80329-X](https://doi.org/10.1016/S0010-8545(00)80329-X).
- Teja, A.S. and Koh, P.Y. (2009), “Synthesis, properties, and applications of magnetic iron oxide nanoparticles”, *Prog. Cryst. Growth Charact. Mater.*, **55**, 22-45.  
<https://doi.org/10.1016/j.pcrysgrow.2008.08.003>.
- Velusamy, S. Roy, A. Sundaram S. and Mallick, T.K. (2021), “A review on heavy metal ions and containing dyes removal through graphene oxide-based adsorption strategies for textile wastewater”, *Treatment Chem. Rec.*, **21**, 1570-1610.  
<https://doi.org/10.1002/tcr.202000153>.
- Wang, Z. Yuan, X. Cheng, Q. Zhang, T. and Luo, J. (2018), “An efficient and recyclable acid-base bifunctional core-shell nanocatalyst for the one-pot deacetalization-Knoevenagel tandemreaction”, *New J. Chem.*, **42**, 11610-11615.  
<https://doi.org/10.1039/C8NJ01934G>.
- Yao, Q. Lu, Z. Zhang, Z. Chen, X. and Lan, Y. (2014), “One-pot synthesis of core-shell Cu@SiO<sub>2</sub> nanospheres and their catalysis for hydrolytic dehydrogenation of ammonia borane and hydrazine borane”, *Sci. Rep.*, **4**, 7597-7605.  
<https://doi.org/10.1038/srep07597>.
- Zare, A. and Barzegar, M. (2020), “Dicationic ionic liquid grafted with silica-coated nano-Fe<sub>3</sub>O<sub>4</sub> as a novel and efficient catalyst for the preparation of uracil-containing heterocycles”, *Res. Chem. Intermed.*, **46**, 3727-3740.  
<https://doi.org/10.1007/s11164-020-04171-2>.
- Zare, A. Sadeghi-Takalo, M. Karimi, M. and Kohzadian, A. (2019), “Synthesis, characterization and application of nano-N,N,N',N'-tetramethyl-N-(silica-*n*-propyl)-N'-sulfo-ethane-1,2-diaminium chloride as a highly efficient catalyst for the preparation of N,N'-alkylidene bisamides”, *Res. Chem. Int.*, **45**, 2999-3018. <https://doi.org/10.1007/s11164-019-03775-7>.
- Zengin, N. Burhan, H. Şavk, A. Göksul, H. and Şen, F. (2020), “Synthesis of benzylidenemalononitrile byKnoevenagel condensation through monodisperse carbon nanotube-based NiCu nanohybrids”, *Sci. Rep.*, **10**, 12758.  
<https://doi.org/10.1038/s41598-020-69764-8>.
- Zhang, S.W. Wang, X.X. Li, J.X. Wen, T. Xu, J.Z. and Wang, X.K. (2014), “Efficient removal of a typical dye and Cr(VI) reduction using N-doped magnetic porous carbon”, *RSC Adv.*, **4**, 63110-63117. <https://doi.org/10.1039/c4ra10189h>.
- Zhang, Y. Zeng, G.M. tang, L. Chen, J. Zhu, Y. He, X.X. and He, Y. (2015), “Electrochemical sensor based on electrodeposited graphene-Au modified electrode and nanoAu carrier amplified signal strategy for attomolar mercury detection”, *Anal. Chem.*, **87**, 989-996. <https://doi.org/10.1021/ac503472p>.
- Zou, Y. Wang, X. Khan, A. Wang, P. Liu, Y. Alsaedi, A. Hayat, T. and Wang, Z. (2016), “Environmental remediation and application of nanoscale zero-valent iron and its composites for the removal of heavy metal ions: A review”, *Environ. Sci. Technol.*, **50**, 7290-7304.  
<https://doi.org/10.1021/acs.est.6b01897>.

CC